The Journal of Infectious Diseases

MAJOR ARTICLE

B-Cell Responses in Hospitalized Severe Acute Respiratory Syndrome Coronavirus 2–Infected Children With and Without Multisystem Inflammatory Syndrome

Nadine Peart Akindele,[1,2,a] Lisa Pieterse,[2] San Suwanmanee,[2,b] and Diane E. Griffin[2]

[1]Division of Pediatric Infectious Diseases, Department of Pediatrics, Johns Hopkins University School of Medicine, Baltimore, Maryland, USA, and [2]W. Harry Feinstone Department of Molecular Microbiology and Immunology, Johns Hopkins Bloomberg School of Public Health, Baltimore, Maryland, USA

Multisystem inflammatory syndrome in children (MIS-C) can complicate infection with severe acute respiratory syndrome coronavirus 2 (SARS-CoV-2), but differences in the immune responses during MIS-C compared to coronavirus disease 2019 (COVID-19) are poorly understood. We longitudinally compared the amounts and avidity of plasma anti-nucleocapsid (N) and spike (S) antibodies, phenotypes of B cells, and numbers of virus-specific antibody-secreting cells in circulation of children hospitalized with COVID-19 (n = 10) and with MIS-C (n = 12). N-specific immunoglobulin G (IgG) was higher early after presentation for MIS-C than COVID-19 patients and avidity of N- and S-specific IgG at presentation did not mature further during follow-up as it did for COVID-19. Both groups had waning proportions of B cells in circulation and decreasing but sustained production of virus-specific antibody-secreting cells for months. Overall, B-cell responses were similar, but those with MIS-C demonstrated a more mature antibody response at presentation compared to COVID-19, suggesting a postinfectious entity.

Keywords. antibody-secreting cells; COVID-19; flow cytometry; antiviral antibody; antibody avidity.

Children infected with severe acute respiratory syndrome coronavirus 2 (SARS-CoV-2) are often only mildly symptomatic, but the recognition of multisystem inflammatory syndrome in children (MIS-C) has called attention to the more severe pediatric clinical manifestations associated with the virus [1–4]. MIS-C is characterized by signs and symptoms reflective of intense immune activation with evidence of increased cytokine production similar to that seen in adults with severe and life-threatening forms of coronavirus disease 2019 (COVID-19) [5–10]. Seropositivity at the time of symptom onset suggests that MIS-C is a post–SARS-CoV-2 inflammatory disease [9]. This possibility is supported by antiviral antibody patterns at the time of hospitalization that show low levels of antiviral immunoglobulin M (IgM) and abundant immunoglobulin G (IgG) similar to those of adult COVID-19 patients convalescent from mild disease [11] but lower than after severe COVID-19 [12]. Compared to healthy donors or mildly ill patients, MIS-C patients have more activated natural killer cells, plasmablasts, and monocyte-activating SARS-CoV-2 IgG [13–15].

Systemic viral infections often lead to a sustained immune response with maintenance of protective titers of neutralizing antibody that correlate with resistance to reinfection [16, 17]. Studies of common cold coronaviruses reveal transient immune memory, and studies of adults infected with other betacoronaviruses causing severe respiratory infection, such as severe acute respiratory syndrome and Middle East respiratory syndrome, indicate that antibody wanes and memory B cells are only present for a few years after recovery in those with mild disease [18–21]. However, data from adults suggest that more severely affected COVID-19 patients develop higher and more durable titers of virus-specific antibody [22–24]. One method of evaluating sustained production of antibody associated with a durable immune response is assessment of antibody-secreting cell (ASC) production. Germinal center–matured ASCs can develop into bone marrow–resident long-lived plasma cells and memory B cells capable of providing durable protective immunity [25–29]. The continued presence of virus-specific ASCs in the peripheral blood is indicative of prolonged output from germinal centers in lymphoid tissue and associated with a durable antibody response [30, 31].

Few studies have compared antiviral immune responses of similarly ill, previously healthy children hospitalized with MIS-C to those hospitalized with severe COVID-19. In addition,

Received 11 February 2022; editorial decision 29 March 2022; accepted 15 April 2022; published online 18 April 2022.

Present affiliations: [a]United States Food and Drug Administration, Silver Spring, Maryland, USA

[b]Princess Srisavangavadhana College of Medicine, Chulabhorn Royal Academy, Bangkok, Thailand.

Correspondence: Diane E. Griffin, MD, PhD, Johns Hopkins Bloomberg School of Public Health, 615 N Wolfe St, Rm E5636, Baltimore, MD 21205, USA (dgriffi6@jhu.edu).

The Journal of Infectious Diseases® 2022;226:822–32

https://doi.org/10.1093/infdis/jiac119

longitudinal data are not available on the humoral immune response or the durability of the immune response in children with MIS-C compared to severe COVID-19. Additionally, data are not available for SARS-CoV-2–infected children, and concerns about the possibility of recurrent episodes of MIS-C upon reinfection with SARS-CoV-2 remain. While an increased presence of plasmablasts in acute MIS-C and children with COVID-19 has been demonstrated [15], determining the continued production of ASCs over time and the specificity of the antibody produced by these cells will provide insight into immune responses and protection in pediatric patients with MIS-C as compared to those with acute COVID-19.

Here, we use enzyme-linked immunosorbent spot (ELISpot) assays and document the plasma levels of virus-specific IgG, IgM and immunoglobulin A (IgA), the avidity of the IgG antibody, and the B-cell subset phenotypes in pediatric patients hospitalized with acute COVID-19 and MIS-C collected longitudinally. These studies suggest that infection had been more prolonged at the time of hospitalization for children with MIS-C than severe COVID-19, but that virus-specific antibody and B-cell responses were otherwise similar.

MATERIALS AND METHODS

Study Participants

Patients admitted with suspected SARS-CoV-2 infection to the Johns Hopkins Hospital were prospectively enrolled into a cohort study entitled "Clinical Characterization Protocol for Severe Emerging Infections." After informed consent, 80 pediatric participants were enrolled between 10 April 2020 to 22 January 2021. Mean time from admission to enrollment into the study was 3.1 days. After hospital discharge, patients were followed and sampled at 1, 3, and 6 months from study entry, within a predefined window of time.

Samples

Peripheral blood was collected in acid citrate dextrose tubes from 53 of those enrolled and peripheral blood mononuclear cells (PBMCs) were isolated using Ficoll-Paque gradients, cryopreserved in fetal bovine serum (FBS) containing 10% dimethyl sulfoxide, and stored in liquid nitrogen as part of the Johns Hopkins Biospecimen Repository. Plasma was frozen at –20°C and used for the previously reported analysis of cytokines and chemokines [5] and of antibody in this study. Sufficient PBMCs were available in 53 samples from 22 patients (10 COVID-19; 12 MIS-C) for analysis at 2–3 postentry time points. Studies were performed according to protocols approved by the Johns Hopkins School of Medicine Institutional Review Board.

SARS-CoV-2 Viral Protein Antigen Preparation

Protein antigens for antibody-binding assays were prepared from lysates of cells expressing native SARS-CoV-2 N and S proteins as previously described [24]. In brief, the HEK293F cell line Ftet2 expressing rtTAv16 [32] was transfected with plasmids expressing a doxycycline-inducible codon-optimized SARS-CoV-2 N open reading frame (ORF) (pCG144), S ORF (pCG146), or empty plasmid. The S protein matches the original SARS-CoV-2 isolate [33], except for 2 proline substitutions that stabilize the trimeric prefusion conformation (986KV987 to 986PP987) and 3 substitutions that eliminate basic amino acids at the S1/S2 cleavage site (682RRAR685 to 682GSAG685). Cells were induced with doxycycline and lysates for use as antigen prepared with 3 freeze-thaw cycles, clarified, and stored at –80°C. Protein coating concentrations were optimized for sensitivity and specificity using prepandemic plasma, COVID-19 convalescent plasma, and control lysates.

Enzyme Immunoassays and Avidity Determination

Enzyme immunoassays (EIAs) and avidity determinations were optimized and performed as previously described [24, 31]. In brief, plasma antibody was quantified with indirect EIAs using clear Nunc Maxisorp 96-well plates (Thermo Fisher Scientific) coated with protein lysates from HEK-293 Ftet2 cells expressing S, N, or no viral protein diluted in phosphate-buffered saline (PBS) pH 7.4 (S lysate) or 50 mM bicarbonate buffer pH 9.6 (N lysate). After coating overnight with 2 µg lysate/mL at 4°C, plates were washed with PBS containing 0.05% Tween20 (PBST) and blocked at room temperature (RT) with nonfat milk in PBST (5% and 3 hours for N; 3% and 1 hour for S). For measurement of IgM, plasma samples were preincubated with protein G agarose (Pierce, catalog number 20398, Thermo Scientific) to deplete IgG. Plasma was serially diluted 2-fold from 1:50 to 1:102 400 and 50 µL was added to each well. Plates were incubated at RT for 2 hours, then washed with PBST. Horseradish peroxidase (HRP)–conjugated secondary antibodies were goat anti-human: IgG (catalog number Ab6858, Abcam, Cambridge, UK; 1:5000), IgM (µ-chain-specific, catalog number A6907, Abcam), and IgA (α-chain-specific, Sigma-Aldrich; 1:3000) with incubation for 1 hour at 37°C. OptEIA TMB substrate (catalog number 555214, BD Biosciences) was added and incubated at RT in the dark for 15 minutes before adding 2 M sulfuric acid as a stop solution. The plates were read at 450 nm. The titer of antibody was determined as the highest dilution with an optical density (OD) 3 times greater than control.

For analysis of IgG avidity, EIAs were performed as above and after plasma incubation (1:50 dilution), wells were washed with PBST and increasing concentrations (0.5–7 M) of ammonium thiocyanate (NH_4SCN) were added for 15 minutes to disrupt the antigen-antibody interaction [34]. Plates were washed, incubated with HRP-conjugated secondary anti-IgG, and processed as above. Avidity index was expressed as the concentration of NH_4SCN required to remove 50% of the bound antibody. Samples with OD values <0.3 were excluded.

ELISpot Assays

MultiScreen-IP 96-well plates (Merck Millipore, Darmstadt, Germany) were coated at 4°C overnight with 10 µg/mL N lysate, S lysate, or immunoglobulin capture antibody (catalog number 609-101-130, Rockland, Limerick, Pennsylvania). Plates washed with PBST were blocked with 10% FBS in RPMI for 2 hours at 37°C. PBMCs were thawed, washed, and resuspended in RPMI-1640 supplemented with 2 mM L-glutamine, 100 U/mL penicillin, 100 µg/mL streptomycin and 10% heat-inactivated FBS. Cells were transferred to blocked/coated plates, incubated 5 hours at 37°C, and then recovered for flow cytometry. Washed plates were incubated with HRP-conjugated secondary antibody to IgM, IgG, and/or IgA overnight at 4°C, developed with diaminobenzidine substrate (catalog number SK-4100, Vector Laboratories) for 20 minutes, and dried, and spots were counted on an automated ELISpot reader (CTL).

B-Cell Phenotypic Analysis by Flow Cytometry

PBMCs washed twice with PBS were stained with Fixable Viability Stain 780 (catalog number 565388, BD Biosciences) to distinguish live/dead cells and blocked using Anti-Hu Fc Receptor Binding Inhibitor (catalog number 14-9161-73, eBioscience, Invitrogen) for 15 minutes. The following antibody staining panel was used: anti-CD3 (SK7)/anti-CD14 (MΦP9)/CD16 (3G8)-APC-Cy7 as a "dump" channel; immunoglobulin D (IgD) (IA6-2)-PE-Cy™7, CD20 (2H7)-BV510, CD138 (MI15)-BV421 (all from BD Biosciences); and CD19 (HIB19)-PE, CD27 (M-T271)-FITC, CD38 (HIT2)-PerCP/Cyanine 5.5 (all from BioLegend). PBMCs were evaluated for presence of total B cells ($CD3^-CD14^-CD16^-CD19^+$), naive B cells ($CD19^+IgD^+CD27^-$), double-negative extrafollicular plasmablasts ($CD19^+IgD^-CD27^-$), and ASCs ($CD19^+CD38^{hi}CD27^{hi}$), as well as plasmablasts ($CD19^+CD27^+CD38^+CD138^-$), plasma cells ($CD19^+CD27^+CD38^{hi}CD138^{hi}$), unswitched memory ($CD19^+CD27^+IgD^+$), and switched memory ($CD19^+CD27^+IgD^-$). Cells were stained in FACS buffer (2% bovine serum albumin and 2 mM ethylenediaminetetraacetic acid in PBS) on ice for 30 minutes, washed 3 times, and fixed with 4.2% formaldehyde BD Cytofix/Cytoperm (catalog number 554714, BD Biosciences) for 20 minutes at 4°C. Data were acquired on a FACSCanto II with FACSDiva Software (BD Biosciences) and analyzed using FlowJo software (Treestar, Ashland, Oregon). Gating strategy was based on fluorescence minus 1 stain control as previously described [24]. The percentages of phenotypic B cells were calculated and converted to cell numbers per microliter based on the absolute lymphocyte count.

Data Analysis

All data were analyzed with 2-way analysis of variance and were considered significant when the *P* value was < .05. Figures were generated with GraphPad Prism 8.4.3 software.

Study Approval

The study was approved by the Johns Hopkins Medicine Institutional Review Board. After informed consent, blood samples were collected in coordination with routine medical care and/or remnant blood samples were retrieved from the clinical laboratory.

RESULTS

Demographics

Of the 53 participants with blood samples collected, 22 had longitudinal samples with sufficient PBMCs for analysis. These patients were confirmed to have SARS-CoV-2 infection by positive nucleic acid amplification test, positive IgG on the Euroimmune (Mountain Lakes, New Jersey) or in-house SARS-CoV-2 EIA, or history of exposure to a known COVID-19 contact in the preceding 4 weeks. The mean age was 10.8 ± 6.4 years, and 55% (n = 12) met the Centers for Disease Control and Prevention criteria for MIS-C: <21 years of age with fever, laboratory evidence of inflammation, severe illness requiring hospitalization, involvement of ≥2 organ systems, no alternative plausible diagnoses, and positive for current/recent SARS-CoV-2 infection [3]. The remaining 45% (n = 10) were categorized as acute COVID-19. Range of days of available longitudinal plasma and PBMC samples was from 1 to 337 days (~11 months) from onset of symptoms. Additional demographic and laboratory data are summarized in Table 1 and Supplementary Tables 1 and 2.

SARS-CoV-2 N- and S-Specific IgM, IgA, and IgG and IgG Avidity

SARS-CoV-2–specific antibody was measured on 28 plasma samples from patients with MIS-C (2–268 days from symptom onset; mean, 59 ± 78 days; median, 33.5 days) and 25 samples from patients with acute COVID-19 (1–337 days from symptom onset; mean, 76 ± 90 days; median, 38 days) by EIA using lysates from cells producing native forms of S or N protein as antigen (Supplementary Figure 1 and Figure 1). IgM and IgA data are reported as OD values (Supplementary Figure 1) and IgG data as titers defined as the reciprocal of highest dilution of plasma with an OD 3 times background (Figure 1). N-specific IgM peaked at similar times between 8 and 21 days from symptom onset (Supplementary Figure 1*A*). S-specific IgM levels were also similar in both groups, with a peak for MIS-C at days 22–42 from symptom onset (Supplementary Figure 1*B*). In both groups and for both antigens, levels of IgM were very low after 42 days from illness onset. N-specific IgA followed a similar trend to N-specific IgM, peaking at 8–21 days in those with MIS-C (Supplementary Figure 1*C*). S-specific IgA levels were also similar between the 2 groups (Supplementary Figure 1*D*). Patients with MIS-C had higher levels of N-specific IgG early (days 0–42) after symptom onset (Figure 1A), whereas S-specific IgG levels were not significantly different from those of patients with acute COVID-19

Table 1. Demographic Characteristics

Characteristic	Total Cohort (N = 22)	MIS-C (n = 12)	Acute COVID-19 (n = 10)	*P* Value
Age, y, median (IQR)	12.52 (4.41–17.19)	9.19 (5.1–14.14)	17.24 (2.35–17.49)	.209
Age, y, mean (SD)	10.82 (6.37)	9.43 (5.46)	11.99 (8.04)	
Race				
Black	6 (27)	3 (25)	3 (30)	
White	5 (23)	1 (8)	4 (40)	
Asian	2 (9)	1 (8)	1 (10)	
Other	9 (41)	7 (58)	2 (20)	
Hispanic ethnicity	10 (45)	8 (67)	2 (20)	
Male sex	10 (45)	7 (58)	3 (30)	.231
Positive SARS-CoV-2 NAT	14 (64)	9 (75)	5 (50)	.378
Duration of symptoms prior to initial (D0) sampling, d, median (IQR)	6.5 (4–10.25)	6 (4.0–10)	8 (2.75–20)	.661
Duration of symptoms prior to initial (D0) sampling, d, mean (SD)	9.23 (9.05)	7.25 (4.03)	12.63 (14.06)	
Duration of symptoms prior to longitudinal timepoints, d, median (IQR)	37.00 (9.50–90.50)	33.5 (7.0–61.5)	38.0 (9.5–110.0)	.599
Duration of symptoms prior to longitudinal timepoints, d, mean (SD)	66.89 (83.15)	59.14 (77.73)	75.56 (89.64)	
Length of stay, d, median (IQR)	6 (4.5–9)	7 (4.3–9)	5 (3–9)	.551
Length of stay, d, mean (SD)	6.90 (4.07)	7.08 (3.29)	7 (5.89)	
ICU	14 (64)	9 (75)	5 (50)	.378
Supplemental oxygen	9 (41)	6 (50)	3 (30)	.415
Intubated	0 (0)	0 (0)	0 (0)	>.999
Vasopressors	6 (27)	5 (42)	1 (10)	.162
Treatment provided	12 (55)	10 (83)	2 (20)	**.008**
Readmission	2 (9)	0 (0)	2 (20)	.195
Death	0 (0)	0 (0)	0 (0)	

Data are presented as No. (%) unless otherwise indicated. Bold font indicates significant difference.

Abbreviations: COVID-19, coronavirus disease 2019; D0, day 0; ICU, intensive care unit; IQR, interquartile range; MIS-C, multisystem inflammatory syndrome in children; NAT, nucleic acid test; SARS-CoV-2, severe acute respiratory syndrome coronavirus 2; SD, standard deviation.

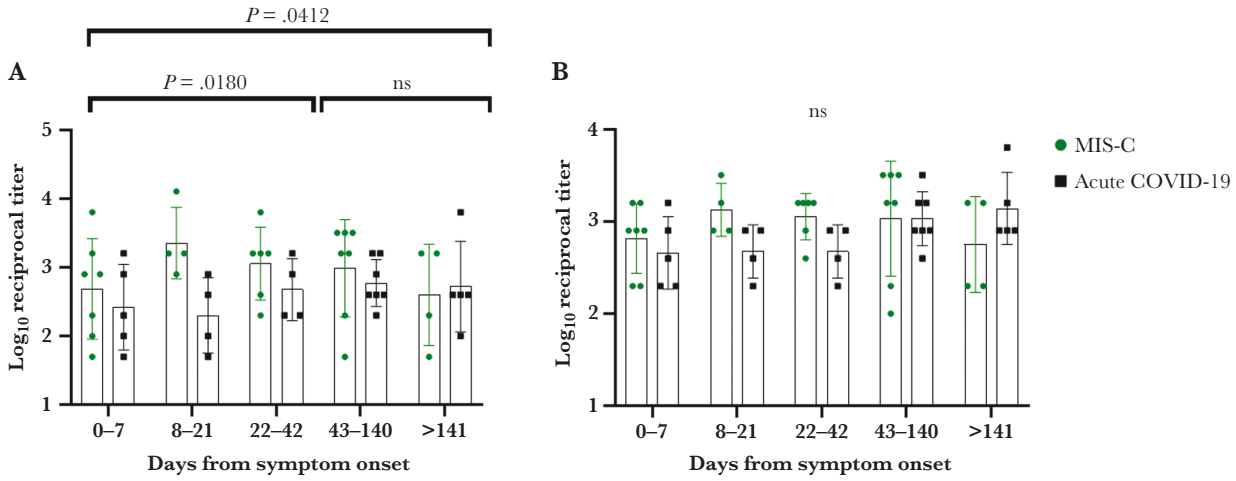

Figure 1. Amounts of severe acute respiratory syndrome coronavirus 2 N- and S-specific immunoglobulin G (IgG) in plasma of multisystem inflammatory syndrome and acute coronavirus disease 2019 pediatric patients as measured by enzyme immunoassay. Data were grouped into time categories based on reported date of symptom onset. *A*, Anti-N IgG. *B*, Anti-S IgG. Data are reported as the $\log_{10}$ reciprocal of the highest dilution with an optical density (450 nm) 3 times background. Abbreviations: COVID-19, coronavirus disease 2019; MIS-C, multisystem inflammatory syndrome in children; ns, not significant.

(Figure 1B). While early timepoints (days 0–42 postinfection) were evaluated separately for all immunoglobulins, only N-specific IgG showed a significant difference.

Avidity of IgG to both N and S proteins was measured by determining the concentration of the chaotropic agent NH_4SCN required to disrupt antibody binding by 50% (Figure 2A and 2B).

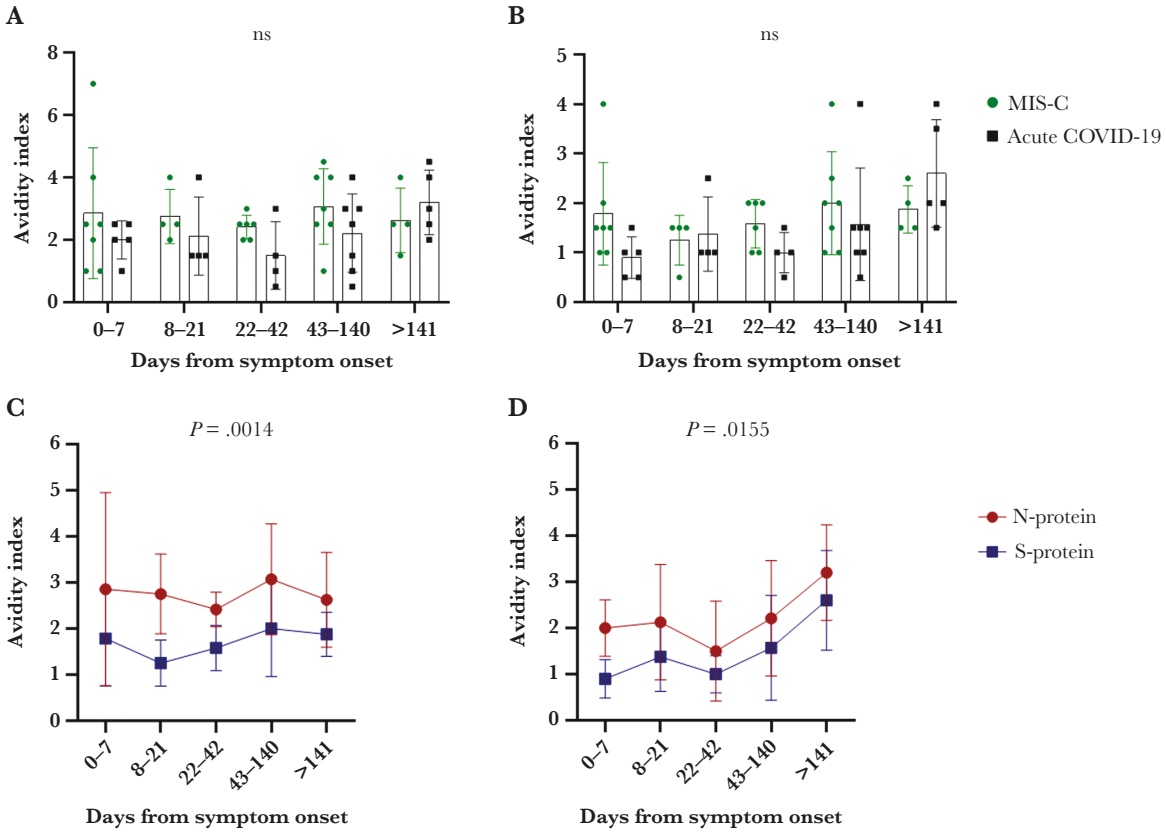

Figure 2. Avidity of severe acute respiratory syndrome coronavirus 2 N- and S-specific immunoglobulin G (IgG) in plasma of multisystem inflammatory syndrome (MIS-C) and acute coronavirus disease 2019 (COVID-19) pediatric patients. Avidity index was defined as the molar concentration of ammonium thiocyanate required to decrease antibody binding by 50%. *A*, Avidity of N-specific IgG. *B*, Avidity of S-specific IgG. Bars indicate the mean and standard deviation (SD) at each timepoint. Comparisons of the mean and SD of avidities of N-specific (circles) and S-specific (squares) IgG for patients with MIS-C (*C*) and acute COVID-19 (*D*). Abbreviations: COVID-19, coronavirus disease 2019; MIS-C, multisystem inflammatory syndrome in children; ns, not significant.

Avidity did not change over time in those with MIS-C (Figure 2C), while those with acute COVID-19 showed increasing avidity from 2 to 5 months after symptom onset (Figure 2D). Mean S-specific avidity was lower than mean N-specific avidity at all time points in both groups (MIS-C, $P = .0014$; acute COVID-19, $P = .0155$).

ASCs Producing N- and S-Specific IgM, IgA, and IgG

SARS-CoV-2–specific ASCs were detected in all hospitalized children at some point after infection (Figure 3). IgM-secreting N- and S-specific ASCs were present primarily before 22 days in both groups (Figure 3A and 3B). IgA-secreting N- and S-specific ASCs were overall similar between the groups with continued production through late timepoints (Figure 3C and 3D). IgG-secreting N- and S-specific ASCs were present at similar levels in those with MIS-C and acute COVID-19 and continued to be detectable more than 4–5 months after symptom onset (Figure 4A and 4B). Total IgG-, IgA-, and IgM-secreting ASCs were essentially unchanged over time and similar in both groups (Figure 4C).

Flow Cytometry Analysis of Changes in B-Cell Subsets in Response to SARS-CoV-2 Infection

Flow cytometry was performed to better characterize the B-cell population phenotypes in the SARS-CoV-2–infected children in this cohort (Figures 5 and 6). The proportion of live cells that were B cells was similar in both groups, with the highest proportions in the first 3 weeks after the onset of symptoms followed by a decrease over time (Figure 5A). Analysis of B-cell subsets did not identify significant changes in the proportions of B cells that were naive, antibody-secreting, or memory or in differences between groups (Figures 5B–D and 6A–D).

DISCUSSION

In this longitudinal study of hospitalized SARS-CoV-2–infected pediatric patients with MIS-C or acute COVID-19, we compared the B-cell responses to the S and N viral proteins by evaluating plasma levels of antiviral antibody; maturation of IgG avidity; ASCs producing virus-specific IgM, IgA, and IgG; and B-cell population phenotypes. Overall, the responses were

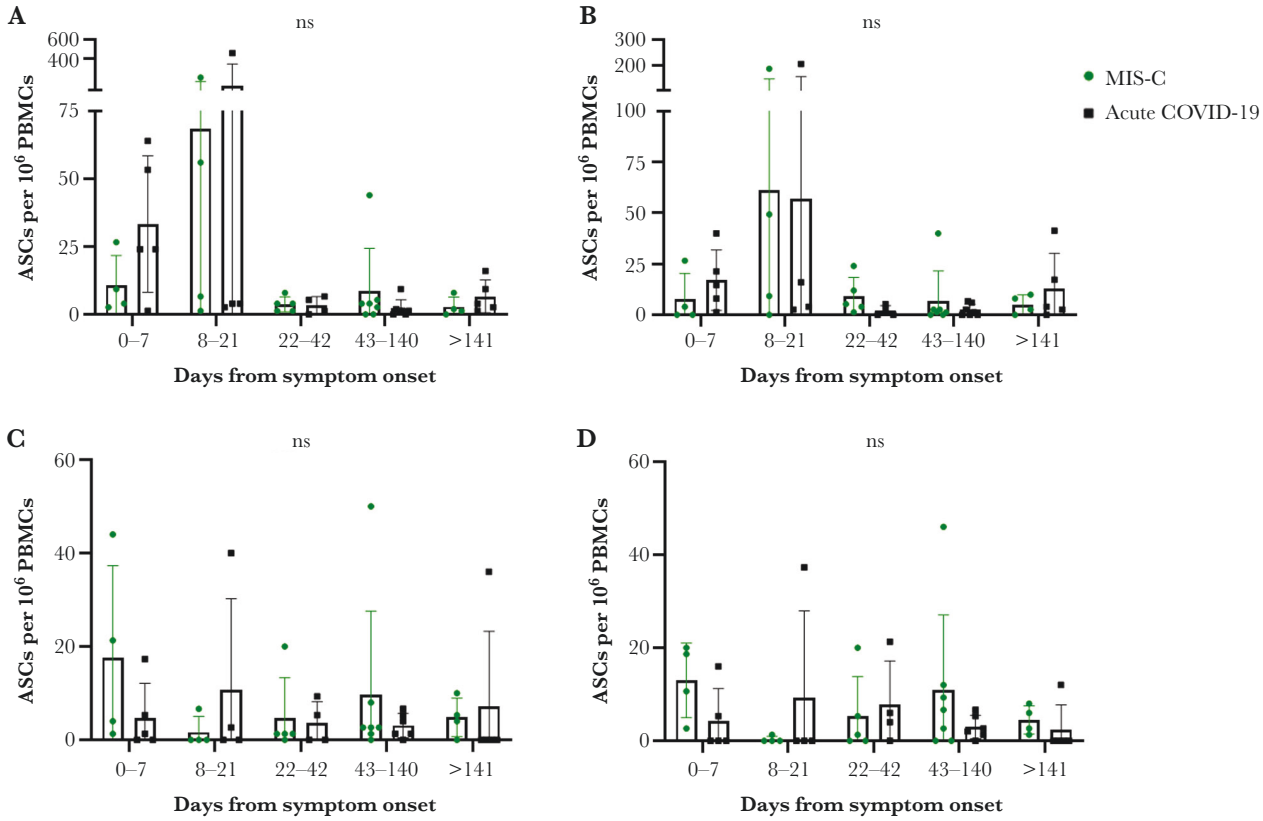

Figure 3. Enzyme-linked immunosorbent spot analyses of virus-specific immunoglobulin M (IgM) and immunoglobulin A (IgA) antibody-secreting cells (ASCs) in circulation. Peripheral blood mononuclear cells (PBMCs) were cultured on plates coated with lysates from cells expressing the N or S protein and stained with antibody to IgM or IgA, and spots were counted. Samples are grouped based on time since symptom onset and ASC data are expressed as spot-forming units/10^6 PBMCs: N-specific IgM (*A*); S-specific IgM (*B*); N-specific IgA (*C*); S-specific IgA (*D*). Abbreviations: ASCs, antibody-secreting cells; COVID-19, coronavirus disease 2019; MIS-C, multisystem inflammatory syndrome in children; ns, not significant; PBMCs, peripheral blood mononuclear cells.

similar with waning proportions of B cells in circulation and decreasing but sustained production of virus N- and S-specific ASCs during recovery from infection. Titers of N-specific IgG were higher early in hospitalization for MIS-C patients than COVID-19 patients. IgG avidity was greater for IgG to N than to S in both groups and at all times examined. For patients with MIS-C, IgG avidity was high at entry and did not mature further during follow-up, whereas for patients with acute COVID-19, avidity of antiviral IgG showed continuing improvement during the 2- to >5-month follow-up. Therefore, MIS-C was associated with a more mature antibody response at the time of hospitalization than acute COVID-19, consistent with a delayed inflammatory response to infection, but long-term production of antiviral antibody was similar.

MIS-C as a postinfection inflammatory syndrome is consistent with the presence of antiviral IgG, elevation of cytokines and chemokines produced by activated myeloid cells, multiorgan damage, and response to immunomodulatory therapy [5–7, 11]. Children with uncomplicated SARS-CoV-2 infection develop IgG antibodies at approximately 1 week from symptom onset with a peak within 2 weeks whereas, as we have observed for N-specific IgG, children with MIS-C have IgG at the time of symptom onset and hospitalization [13, 35]. It has been presumed that this severe phenotype in children might be associated with a more durable immune response as is true for adults with severe COVID-19 compared to mild disease. We evaluated the persistence of antiviral IgG for up to 11 months from symptom onset (range, 1–337 days) and found that antibody to both the S and N proteins was maintained in both groups of children with different manifestations of severe SARS-CoV-2–induced disease.

Plasma antibody levels are maintained by long-lived plasma cells that are produced from germinal centers in secondary lymphoid tissue and reside primarily in bone marrow. Information on production of virus-specific ASCs was obtained using ELISpot assays on PBMCs, and both S- and N-specific IgG-producing ASCs were continuously detected, although in decreasing numbers over time in both groups of children. The persistent appearance of ASCs in the periphery after infection has been associated with greater durability of antibody responses and varies with different viral infections. For example, after acute infection with measles virus, ASC

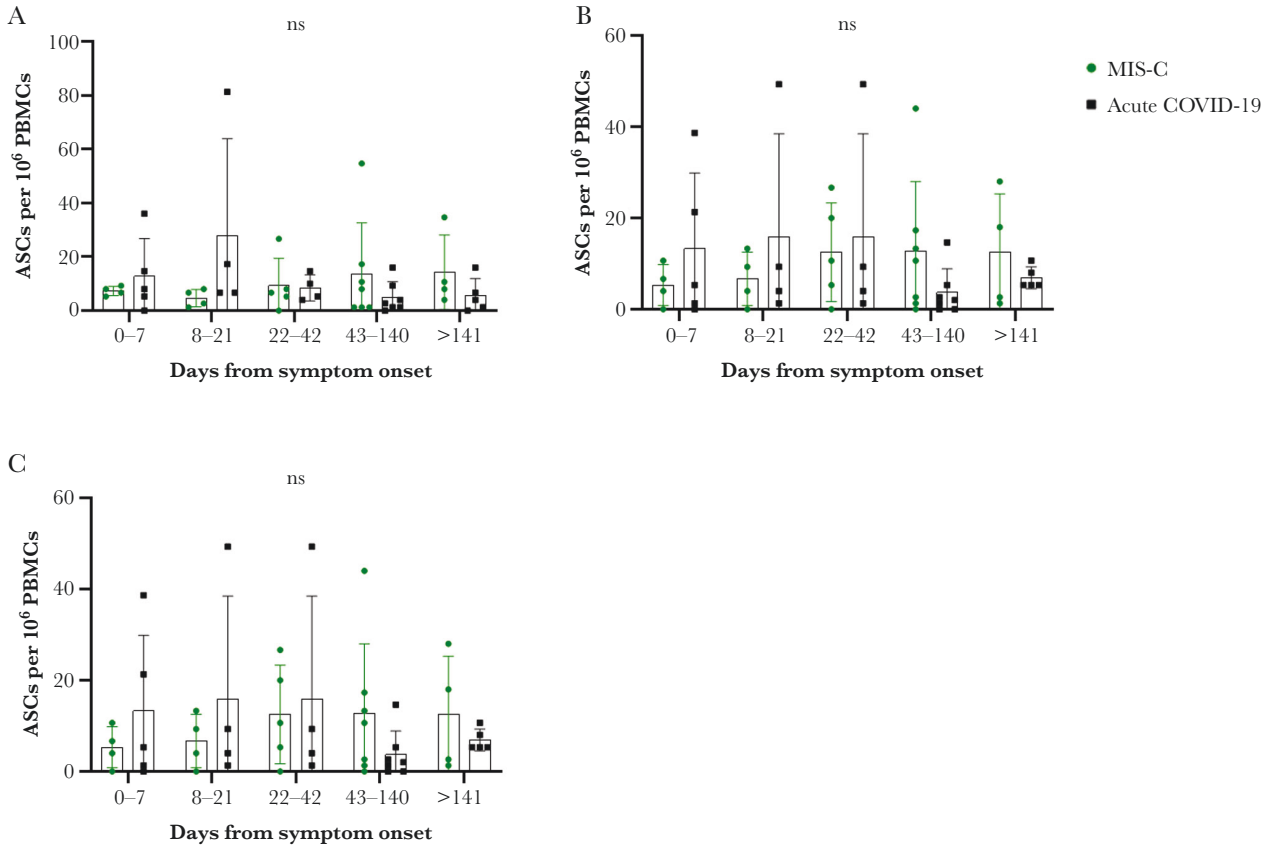

Figure 4. Enzyme-linked immunosorbent spot analyses of total and virus-specific immunoglobulin G (IgG) antibody-secreting cells (ASCs) in circulation. Peripheral blood mononuclear cells (PBMCs) were cultured on plates coated with lysates from cells expressing the N or S protein or antibody to immunoglobulin and stained with antibody to IgG or all immunoglobulins, and spots were counted. Samples are grouped based on time since symptom onset and data are expressed as spot-forming units/10^6 PBMCs: N-specific IgG (*A*); S-specific IgG (*B*); total immunoglobulin M, immunoglobulin A, and IgG ASCs (*C*). Abbreviations: ASCs, antibody-secreting cells; COVID-19, coronavirus disease 2019; MIS-C, multisystem inflammatory syndrome in children; ns, not significant; PBMCs, peripheral blood mononuclear cells.

production is sustained for >5 months from the time of infection and life-long protective immunity is established [17, 31, 36]. In contrast, after infection with respiratory syncytial virus, ASCs can be detected for about 2 months and protection from reinfection is brief [37–40]. Our previous studies of hospitalized adults with SARS-CoV-2 infection showed that those with more severe disease produced more S-specific ASCs than those with mild disease [24], a difference that we did not detect in our small cohort of hospitalized SARS-CoV-2–infected pediatric patients. This is consistent with the hypothesis that MIS-C is a different disease process than severe COVID-19 and may be explained in part by the fact that we did not study nonhospitalized children with mild disease for comparison.

Avidity maturation is a measure of ongoing stimulation of lymphoid tissue that yields B cells selected for improved antigen binding capacity [25]. In SARS-CoV-2–infected adults and children, disease severity is associated with a more pronounced innate immune response [5, 8] that may facilitate a more robust adaptive immune response [41–44], including higher affinity antibody. As previously observed for adults [24, 45, 46], N protein antibody avidity was higher than S protein antibody avidity in SARS-CoV-2–infected children. The presence of high avidity in children with MIS-C at the time of hospitalization compared to the ongoing maturation in children with acute COVID-19 is consistent with MIS-C as a postinfectious condition.

Flow cytometry helps to better define the B-cell populations in pediatric as well as adult patients infected with SARS-CoV-2. Adult patients with severe COVID-19 have higher percentages of flow cytometry–defined ASCs, plasmablasts, and plasma cells in circulation [24]. Few studies have evaluated the B-cell populations in children with MIS-C compared to acute COVID-19. In cross-sectional studies of acute MIS-C patients compared to healthy children, plasmablasts and naive B cells are increased and memory B cells reduced [15], and a comparison of MIS-C and acute COVID-19 pediatric patients showed that plasmablast frequencies were similar and higher than in healthy adults [14]. In our hospitalized pediatric cohort, we noted a decrease in circulating B cells over time, but did not identify differences in the B-cell subsets for MIS-C compared to acute COVID-19.

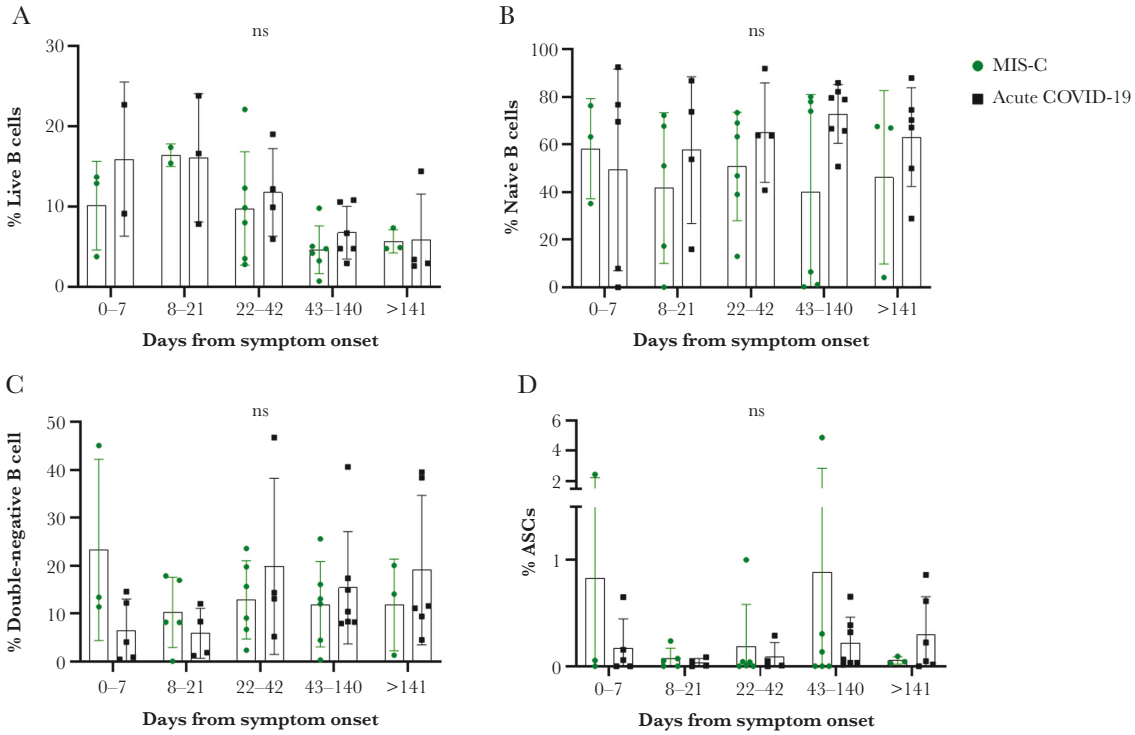

Figure 5. Flow cytometry analyses of B-cell populations in circulation. Results are grouped by days since symptom onset and analyzed as the percentages of cells for each subset. *A*, CD19$^+$ B cells as a percentage of total lymphocytes. *B*, Naive B cells as a percentage of CD19$^+$ lymphocytes. *C*, Double-negative B cells as a percentage of CD19$^+$ lymphocytes. *D*, Antibody-secreting cells as a percentage of CD19$^+$ lymphocytes. Abbreviations: ASCs, antibody-secreting cells; COVID-19, coronavirus disease 2019; MIS-C, multisystem inflammatory syndrome in children; ns, not significant.

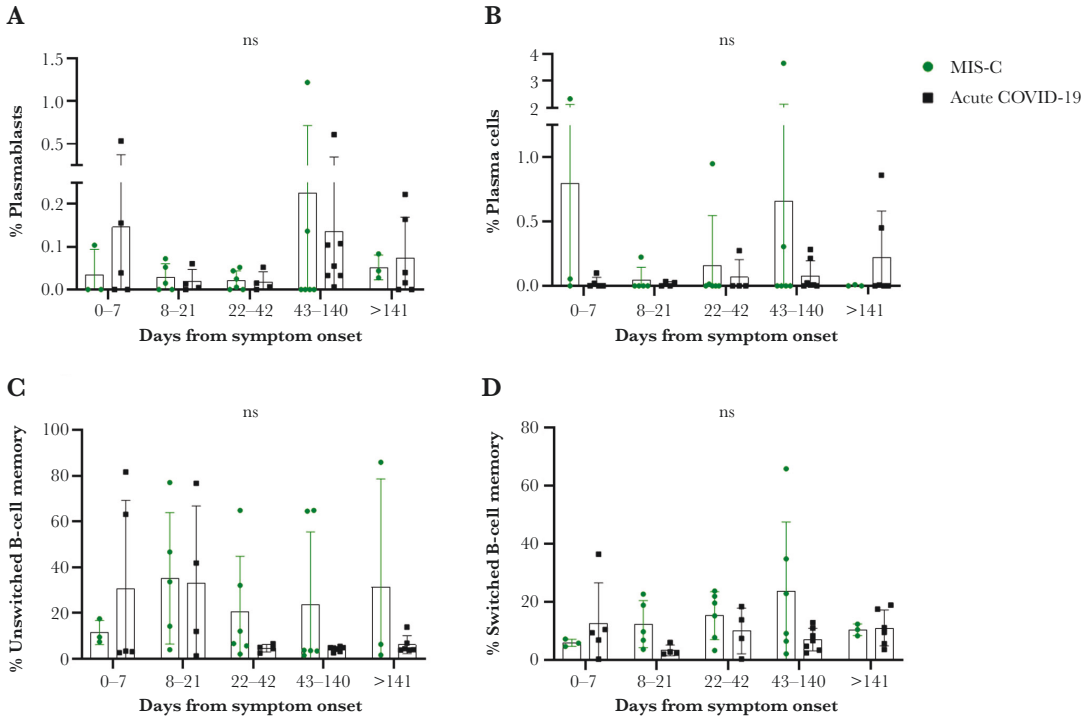

Figure 6. Flow cytometry analyses of B-cell populations in circulation. Results are grouped by days since symptom onset and analyzed as the percentages of cells for each subset. *A*, Plasmablasts as a percentage of CD19$^+$ lymphocytes. *B*, Plasma cells as a percentage of CD19$^+$ lymphocytes. *C*, Unswitched memory B cells as a percentage of CD19$^+$ lymphocytes. *D*, Switched memory B cells as a percentage of CD19$^+$ lymphocytes. Abbreviations: COVID-19, coronavirus disease 2019; MIS-C, multisystem inflammatory syndrome in children; ns, not significant.

Our study has limitations. The sample size is small due to the rarity of MIS-C as well as the complexity of coordinating follow-up for pediatric patients during the peak of the pandemic. Therefore, it is difficult to apply our findings to the broader population of children affected by this disease. Additionally, we did not study the neutralizing capacity of the antibodies and do not have sequence information on the infecting viruses. Furthermore, we were not able to correlate the longitudinal data with clinical symptoms after hospital discharge or determine the protection from reinfection.

In summary, pediatric patients hospitalized with MIS-C had evidence of a more mature antiviral antibody response with more anti-N IgG and maximal avidity maturation at the time of admission than those with acute COVID-19. Predicted durability of the antiviral antibody response was similar with continued production of virus-specific ASCs for months after infection. Further study is required to determine the relationship of type of clinical disease to the durability of protective immunity in children.

Supplementary Data

Supplementary materials are available at *The Journal of Infectious Diseases* online. Supplementary materials consist of data provided by the author that are published to benefit the reader. The posted materials are not copyedited. The contents of all supplementary data are the sole responsibility of the authors. Questions or messages regarding errors should be addressed to the author.

Notes

Author contributions. N. P. A. and D. E. G. designed the study. N. P. A., L. P., and S. S. performed the experiments. N. P. A. and D. E. G. wrote the manuscript with help from L. P. and S. S.

Acknowledgments. We thank Dr Deborah Persaud for establishing the pediatric cohorts, Christine Atik for assisting with retrieving participant laboratory data, Debra Hauer for laboratory assistance, and Dr Stephen Gould and Chenxu Guo for supplying lysates of N and S protein–producing cells.

Disclaimer. The views expressed in this article are those of the authors and do not necessarily represent the views of the US Food and Drug Administration or the US government.

Financial support. The specimens utilized were part of the Johns Hopkins University Biospecimen Repository, which is based on the contribution of many patients, research teams, and clinicians and supported by a Johns Hopkins University Provost Research Grant. This research work was funded by the Johns Hopkins COVID-19 Research Response Program (grant to D. E. G.); a scholarship in commemoration of Her Royal Highness Princess Chulabhorn's 60th Birthday Anniversary, Chulabhorn Royal Academy (to S. S.); the National Institutes of Health (grant number T32-AI052071 to N. P. A.); and the Bauernschmidt Committee of the Eudowood Board at Johns Hopkins School of Medicine (award to N. P. A.).

Potential conflicts of interest. D. G. is on advisory boards for GlaxoSmithKline, Takeda Pharmaceutical, and GreenLight Biosciences. All other authors report no potential conflicts of interest.

All authors have submitted the ICMJE Form for Disclosure of Potential Conflicts of Interest. Conflicts that the editors consider relevant to the content of the manuscript have been disclosed.

REFERENCES

1. Dong Y, Mo X, Hu Y, et al. Epidemiology of COVID-19 among children in China. Pediatrics **2020**; 145:e20200702.
2. Pouletty M, Borocco C, Ouldali N, et al. Paediatric multisystem inflammatory syndrome temporally associated with SARS-CoV-2 mimicking Kawasaki disease (Kawa-COVID-19): a multicentre cohort. Ann Rheum Dis **2020**; 79:999–1006.
3. Feldstein LR, Rose EB, Horwitz SM, et al. Multisystem inflammatory syndrome in U.S. children and adolescents. N Engl J Med **2020**; 383:334–46.
4. McCrindle BW, Manlhiot C. SARS-CoV-2-related inflammatory multisystem syndrome in children: different or shared etiology and pathophysiology as Kawasaki disease? JAMA **2020**; 324:246–8.
5. Peart Akindele N, Kouo T, Karaba AH, et al. Distinct cytokine and chemokine dysregulation in hospitalized children with acute coronavirus disease 2019 and multisystem inflammatory syndrome with similar levels of nasopharyngeal severe acute respiratory syndrome coronavirus 2 shedding. J Infect Dis **2021**; 224:606–15.
6. Carter MJ, Fish M, Jennings A, et al. Peripheral immunophenotypes in children with multisystem inflammatory syndrome associated with SARS-CoV-2 infection. Nat Med **2020**; 26:1701–7.
7. Consiglio CR, Cotugno N, Sardh F, et al. The immunology of multisystem inflammatory syndrome in children with COVID-19. Cell **2020**; 183:968–81.e7.
8. Karaba AH, Zhou W, Hsieh LL, et al. Differential cytokine signatures of severe acute respiratory syndrome coronavirus 2 (SARS-CoV-2) and influenza infection highlight key differences in pathobiology. Clin Infect Dis **2022**; 74:254–62.
9. Feldstein LR, Tenforde MW, Friedman KG, et al. Characteristics and outcomes of US children and adolescents with multisystem inflammatory syndrome in children (MIS-C) compared with severe acute COVID-19. JAMA **2021**; 325:1074–87.
10. Whittaker E, Bamford A, Kenny J, et al. Clinical characteristics of 58 children with a pediatric inflammatory

multisystem syndrome temporally associated with SARS-CoV-2. JAMA **2020**; 324:259–69.
11. Gruber CN, Patel RS, Trachtman R, et al. Mapping systemic inflammation and antibody responses in multisystem inflammatory syndrome in children (MIS-C). Cell **2020**; 183:982–95.e14.
12. Weisberg SP, Connors TJ, Zhu Y, et al. Distinct antibody responses to SARS-CoV-2 in children and adults across the COVID-19 clinical spectrum. Nat Immunol **2021**; 22:25–31.
13. Bartsch YC, Wang C, Zohar T, et al. Humoral signatures of protective and pathological SARS-CoV-2 infection in children. Nat Med **2021**; 27:454–62.
14. Vella LA, Giles JR, Baxter AE, et al. Deep immune profiling of MIS-C demonstrates marked but transient immune activation compared to adult and pediatric COVID-19. Sci Immunol **2021**; 6:eabf7570.
15. Ramaswamy A, Brodsky NN, Sumida TS, et al. Immune dysregulation and autoreactivity correlate with disease severity in SARS-CoV-2-associated multisystem inflammatory syndrome in children. Immunity **2021**; 54:1083–95.e7.
16. Antia A, Ahmed H, Handel A, et al. Heterogeneity and longevity of antibody memory to viruses and vaccines. PLoS Biol **2018**; 16:e2006601.
17. Amanna IJ, Carlson NE, Slifka MK. Duration of humoral immunity to common viral and vaccine antigens. N Engl J Med **2007**; 357:1903–15.
18. Wu LP, Wang NC, Chang YH, et al. Duration of antibody responses after severe acute respiratory syndrome. Emerg Infect Dis **2007**; 13:1562–4.
19. Liu W, Fontanet A, Zhang PH, et al. Two-year prospective study of the humoral immune response of patients with severe acute respiratory syndrome. J Infect Dis **2006**; 193:792–5.
20. Tang F, Quan Y, Xin ZT, et al. Lack of peripheral memory B cell responses in recovered patients with severe acute respiratory syndrome: a six-year follow-up study. J Immunol **2011**; 186:7264–8.
21. Alshukairi AN, Khalid I, Ahmed WA, et al. Antibody response and disease severity in healthcare worker MERS survivors. Emerg Infect Dis **2016**; 22:1113–5.
22. Li K, Huang B, Wu M, et al. Dynamic changes in anti-SARS-CoV-2 antibodies during SARS-CoV-2 infection and recovery from COVID-19. Nat Comm **2020**; 11:6044.
23. Long QX, Tang XJ, Shi QL, et al. Clinical and immunological assessment of asymptomatic SARS-CoV-2 infections. Nat Med **2020**; 26:1200–4.
24. Bartlett ML, Suwanmanee S, Peart Akindele N, et al. Continued virus-specific antibody-secreting cell production, avidity maturation and B cell evolution in patients hospitalized with COVID-19 [manuscript published online ahead of print 14 March 2022]. Viral Immunol **2022**. doi:10.1089/vim.2021.0191.
25. Victora GD, Nussenzweig MC. Germinal centers. Annu Rev Immunol **2012**; 30:429–57.
26. Suan D, Sundling C, Brink R. Plasma cell and memory B cell differentiation from the germinal center. Curr Opin Immunol **2017**; 45:97–102.
27. Takahashi Y, Kelsoe G. Role of germinal centers for the induction of broadly-reactive memory B cells. Curr Opin Immunol **2017**; 45:119–25.
28. Benner R, Hijmans W, Haaijman JJ. The bone marrow: the major source of serum immunoglobulins, but still a neglected site of antibody formation. Clin Exp Immunol **1981**; 46:1–8.
29. Slifka MK, Matloubian M, Ahmed R. Bone marrow is a major site of long-term antibody production after acute viral infection. J Virol **1995**; 69:1895–902.
30. Mesin L, Ersching J, Victora GD. Germinal center B cell dynamics. Immunity **2016**; 45:471–82.
31. Nelson AN, Lin WW, Shivakoti R, et al. Association of persistent wild-type measles virus RNA with long-term humoral immunity in rhesus macaques. JCI Insight **2020**; 5:e1344992.
32. Das AT, Tenenbaum L, Berkhout B. Tet-on systems for doxycycline-inducible gene expression. Curr Gene Ther **2016**; 16:156–67.
33. Zhou P, Yang XL, Wang XG, et al. A pneumonia outbreak associated with a new coronavirus of probable bat origin. Nature **2020**; 579:270–3.
34. Nair N, Moss WJ, Scott S, et al. HIV-1 infection in Zambian children impairs the development and avidity maturation of measles virus-specific immunoglobulin G after vaccination and infection. J Infect Dis **2009**; 200:1031–8.
35. Long QX, Liu BZ, Deng HJ, et al. Antibody responses to SARS-CoV-2 in patients with COVID-19. Nat Med **2020**; 26:845–8.
36. Panum P. Observations made during the epidemic of measles on the Faroe Islands in the year 1846. Med Classics **1938**; 3:829–86.
37. Galanti M, Birger R, Ud-Dean M, et al. Longitudinal active sampling for respiratory viral infections across age groups. Influenza Other Respir Viruses **2019**; 13:226–32.
38. Falsey AR, Singh HK, Walsh EE. Serum antibody decay in adults following natural respiratory syncytial virus infection. J Med Virol **2006**; 78:1493–7.
39. Hall CB, Walsh EE, Long CE, Schnabel KC. Immunity to and frequency of reinfection with respiratory syncytial virus. J Infect Dis **1991**; 163:693–8.
40. Lee FE, Falsey AR, Halliley JL, Sanz I, Walsh EE. Circulating antibody-secreting cells during acute respiratory syncytial virus infection in adults. J Infect Dis **2010**; 202:1659–66.

41. MacLennan IC, Toellner KM, Cunningham AF, et al. Extrafollicular antibody responses. Immunol Rev **2003**; 194:8–18.
42. Shrock E, Fujimura E, Kula T, et al. Viral epitope profiling of COVID-19 patients reveals cross-reactivity and correlates of severity. Science **2020**; 370:eabd4250.
43. Gudbjartsson DF, Norddahl GL, Melsted P, et al. Humoral immune response to SARS-CoV-2 in Iceland. N Engl J Med **2020**; 383:1724–34.
44. Lynch KL, Whitman JD, Lacanienta NP, et al. Magnitude and kinetics of anti-severe acute respiratory syndrome coronavirus 2 antibody responses and their relationship to disease severity. Clin Infect Dis **2021**; 72: 301–8.
45. Qiu M, Shi Y, Guo Z, et al. Antibody responses to individual proteins of SARS coronavirus and their neutralization activities. Microbes Infect **2005**; 7:882–9.
46. Burbelo PD, Riedo FX, Morishima C, et al. Sensitivity in detection of antibodies to nucleocapsid and spike proteins of severe acute respiratory syndrome coronavirus 2 in patients with coronavirus disease 2019. J Infect Dis **2020**; 222:206–13.